STATE OF ILLINOIS
WILLIAM G. STRATTON, *Governor*
DEPARTMENT OF REGISTRATION AND EDUCATION
VERA M. BINKS, *Director*

Hydraulic Fracture Theory

Part III. – Elastic Properties of Sandstone

James M. Cleary

DIVISION OF THE
ILLINOIS STATE GEOLOGICAL SURVEY
JOHN C. FRYE, *Chief* URBANA

CIRCULAR 281 1959

HYDRAULIC FRACTURE THEORY
Part III. – Elastic Properties of Sandstone

James M. Cleary

ABSTRACT

This study, the last of a three-part series, was undertaken primarily to evaluate certain elastic properties of the porous sandstones. Such properties may be used in calculating the changes in underground stresses that take place as pore pressure changes. As the underground stresses control hydraulic fracture propagation, knowledge of these stresses is important in recovery of oil.

Samples of sandstone were subjected to changes in pore pressure and external stresses. The resulting strains were measured by resistance wire gages and the elastic properties computed.

In Parts I and II of the project, the hydraulic fracturing process was examined as a problem in applied mechanics, with particular emphasis on elasticity. It was concluded that hydraulic fracture propagation was controlled mainly by the horizontal stress in the rock and that this stress would change with the pore pressure.

The laboratory data of Part III confirm experimentally the predicted horizontal stress changes. Elastic properties of the sandstone were found to vary with mean effective stress. The regular variation of elastic properties with porosity should allow rough prediction of elastic behavior of a given type of rock on the basis of porosity.

INTRODUCTION

The induction of hydraulic fractures in buried sediments is governed in large part by the stress condition of these sediments. The stress condition is in turn influenced by the pore pressure. The changes in stress and strain resulting from changes in pore pressure are governed by the elastic properties of the material insofar as these changes are reversible. This report describes the elastic behavior of sandstone, or, in other words, the reversible relationships between stress, strain, and pore pressure.

Parts I and II of this study of hydraulic fracture theory were prepared as part of a project set up by the Illinois State Geological Survey, in consultation with the Department of Mining and Metallurgical Engineering of the University of Illinois, to investigate the process and its various elements.

Part I dealt mainly with the adaptation of theories on the mechanics of materials to the problems of hydraulic fracture mechanics and to a description of stress conditions in porous sediments. Part II was concerned with hydraulic fracture mechanics, the orientation, distribution, and possible control of fractures, and the importance of pore pressure.

This final part of the study deals with laboratory experiments suggested by the theoretical studies of the first two sections. Parts I and II concluded that use-

ful calculations bearing on the mechanical aspects of the hydraulic fracturing process can be made if the elastic properties of the porous strata are known. Such calculations would consider the influence of changes in pore pressure on the stress condition of the rock around an oil well.

The elastic properties of porous granular materials are known to change as the state of stress changes. The published literature gives such a diversity of values for elastic properties of rocks that it did not seem practical to use published values for the application considered here. For this reason an experimental investigation was made of the elastic properties of some sandstone samples taken from drill cores. The answers to the following questions were sought in these experiments:

1) What reasonable values of the elastic properties of sandstone, within the range of stress conditions existing in the oil reservoir, can be established?

2) How do these properties change with stress condition?

Acknowledgments

I express appreciation to the Department of Mining and Metallurgical Engineering of the University of Illinois for financing the construction of the apparatus used in the tests; to Professor Walter D. Rose for guidance in performing these experiments; to the Illinois State Geological Survey for providing samples and aiding in the preparation of the manuscript; and to Alfred H. Bell, head of the Oil and Gas Section of the Illinois State Geological Survey, Lester L. Whiting of the same section, Kenneth R. Larson of the Natural Gas Storage Company of Illinois, Professor H. R. Wetenkamp of the Department of Theoretical and Applied Mechanics of the University of Illinois, and William J. McGuire of the Atlantic Refining Company, all of whom assisted in various ways.

This report is adapted from a thesis submitted in partial fulfillment of the requirements for the degree of Master of Science from the University of Illinois, 1959.

NOTATION

Symbols

α = Linear coefficient of thermal expansion, 1/Temp

β = Grain compressibility, in^2/lb

ϵ = Strain

E = Young's modulus, lb/in^2

e = Volume dilatation

J = Linear coefficient of pore pressure expansion, in^2/lb

μ = Poisson's ratio

n = Fractional pore area in a plane through a porous material; the porosity

σ = Total stress with direction unspecified, surface pressure, or mean stress, lb/in^2. When the mean stress, σ , is used as a variable, it is assumed that the stress change is hydro-

static. That is, the changes in each of the three principal stresses are equal.

$\bar{\sigma}$ = Effective stress with direction unspecified, or mean effective stress, lb/in^2. When the mean effective stress is used as a variable there is no restriction on the way in which the principal effective stresses vary individually.

σ_x = Total stress in the x direction, lb/in^2

σ'_x = Solid stress in the x direction, lb/in^2

P = Pore pressure, lb/in^2

X = A constant

$Z = \left[\frac{\delta\sigma_r}{\delta P}\right]_{\substack{\sigma_z = \text{constant} \\ \epsilon_r = \text{constant}}} = \left[\frac{JE}{1-\mu}\right]$ = the rate of change of the horizontal stress with pore pressure for the usual subsurface boundary conditions.

cyclic = Two additional similar equations are obtained by cyclic interchange of the subscripts, implying that the given equation is general for the three coordinate directions.

δ = Differential of

Subscripts:

x, y, z, r = The principal stress directions. When r is used the problem is assumed to have radial symmetry with, for example, $\sigma_x = \sigma_y = \sigma_r$. This is always the condition in the experiments.

o = The initial, or base, value.

PREVIOUS WORK

Adams and Williamson (1923) measured the compressibility of rocks and minerals under high confining pressure in two groups of experiments. For one set of experiments they coated the rock cylinders with tin foil to prevent access of the fluid to the pores. In another set of experiments they exposed the rock cylinders to the pressuring fluid so that the pressure would act throughout the communicating porous structure as well as on the outside surface of the specimen.

They found the compressibilities of minerals and unjacketed rock changed only slightly by pressure. For example, the compressibility of quartz is reduced about 1 percent by a 3,000 psi increase in pressure. They also found that the compressibility of unjacketed rocks could be calculated with good approximation by obtaining the weighted average compressibilities of the constituent mineral grains.

The compressibilities of the jacketed specimens were much greater than the compressibilities of the unjacketed specimens. As pressure increased, the compressibilities of the jacketed samples decreased, rapidly at first, and approached asymptotically the compressibilities of the unjacketed specimens.

Adams and Williamson reasonably explained the initially high value of the compressibilities of jacketed specimens by pointing out that when the fluid is

excluded from the pores the pressure tended to close the pores as well as reduce the grain volume.

Zisman (1933b) studied the compressibility of rocks under moderate confining pressures and observed in greater detail than did Adams and Williamson the change in compressibility of jacketed specimens under confining pressure.

One remarkable thing about this phenomenon of changing bulk compressibility, observed by Adams and Williamson and later by Zisman, was the fact that the rocks being tested were what normally would be considered nonporous and impervious. Most of the rocks tested were igneous. "Nonporous" limestone, sandstone, dolomite, and marble also were included.

Birch and Bancroft (1938) shed further light on the phenomenon of the initially high compressibility of jacketed rocks. They pointed out that an aggregate of anisotropic crystals of random orientation can exist in a hydrostatic state of stress without any porosity under only one set of temperature-pressure conditions. Under any other set of conditions the various crystal grains will tend to expand differently in different directions, developing microscopic unequal stresses that tend to prop open small fissures.

Therefore, when the dense rocks, such as granite and basalt, are removed from the environment of temperature and pressure under which they have become normalized through geologic time, their original dense structure may be loosened slightly by the development of minute fissures. Birch (1943) stated that a slight loosening of structure in rocks would occur with moderate heating.

The existence of these phenomena has probably best been demonstrated in attempts to measure thermal expansion of rocks. Dane (1942) states, "When a rock specimen is measured in the laboratory, it is found that the coefficients of expansion are very different on heating and cooling, with a still different result on each subsequent run. This is due to the unlike expansions of adjacent grains because of differences both of composition and of orientation. As a result, when a rock is heated the grains with the largest thermal dilation tend to determine the apparent change in length of the whole specimen, creating internal fractures or 'pores'."

If such secondary porosity can develop in compact rocks when they are removed from their geologic environment, we must also expect that porous rocks may be disrupted in a similar manner. There also may be additional alteration due to treatment in the laboratory. Therefore, laboratory measurements of the elastic properties of porous rocks placed under low confining pressure may be influenced by secondary disruption of rock structure. However, as the contact area between grains is much smaller for porous sandstones than for dense nonporous rocks, the porous sandstone will have microscopic stresses at areas of grain contact that are much higher than the applied external stress. Hence, moderate confining pressures should be sufficient to remove slack that may have developed in the system owing to removal from the natural environment.

The early workers concerned with elastic properties of rock were interested principally in the interpretation of seismic wave phenomena. Zisman (1933a) compared measured seismic wave velocities in shallow beds with velocities (calculated from statically determined Poisson's ratio, μ, and Young's modulus, E) measured on rock cylinders at atmospheric pressure. He found the experimental determinations of Young's modulus and Poisson's ratio too low to account for seismic wave velocities. Zisman also noted that E and μ increased with the mean applied stress.

Ide (1936) compared static and dynamic measurements of Young's modulus

on rocks at atmospheric pressure. The static measurements of E yielded the lower values.

Ide found a wide discrepancy between static and dynamic measurements in the same rocks and the discrepancies seemed to be greater for the more porous rocks. The present investigation involves only static states of stress in porous rocks and is therefore limited to static measurements.

Birch and Bancroft (1938) measured the shear modulus of dense rocks by the torsional vibration method, carrying their experiment to elevated temperatures and high pressures. Their early work is not applicable to the present problem because the rocks tested were almost without porosity.

Carpenter and Spencer (1941) measured the "compressibility" of high porosity sandstones in an effort to learn whether fluid withdrawal would compress the sandstone sufficiently to account for subsidence observed in certain oil fields. They enclosed cylindrical samples in foil and inserted a tube to connect the porous system of the specimen to the outside of the pressuring cell. As pressure was increased on the exterior of the specimen, the volume of fluid forced from the pores was measured. Carpenter and Spencer's data are converted to an appropriate form and plotted with the new data reported below.

Hall (1953) and Fatt (1958a) measured what they term pore compressibility. Their procedure was similar to that of Carpenter and Spencer but the volume of fluid produced from the specimens resulted from a reduction in the pore pressure rather than an increase in the external stress. Thus Hall and Fatt more closely duplicated reservoir conditions.

In another paper Fatt (1958b) reports measurements of bulk compressibilities on porous sandstones. In his experiments linear strain was measured while hydrostatic pressure was being applied to jacketed cylindrical specimens. He also measured a property he termed "pseudo bulk compressibility," which is essentially the same property measured by Carpenter and Spencer.

Fatt measured another property also obtained in the experimental work reported here. In this report the property is expressed

$$\left[\frac{\delta \sigma}{\delta P}\right]_{\epsilon} = \text{constant} \quad \text{or} \quad \left[\frac{JE}{1-2\mu}\right]$$

and its physical significance is discussed.

Fatt also developed several analytical models, including an extension of the sphere-pack model of Brandt (1955), to rationalize the mechanical behavior of porous rocks.

THEORY

The theory of elasticity of porous materials is here developed briefly. Earlier works cited below cover the subject much more fully.

Biot (1941) developed a theory of elasticity of porous materials in which the compressibility of the pore volume is related to the other deformation constants. Later, Biot (1955) extended his theory to include anisotropy.

Gassmann (1951) also studied pore volume elasticity and the propagation of elastic waves in porous materials.

Geertsma (1957) discussed elastic as well as inelastic compressibility of porous materials. He gives a convenient set of connecting equations relating the bulk and pore compressibilities for various boundary conditions. One of these is used later in this report to convert the data of Carpenter and Spencer to the form

used here.

Lubinski (1954) discussed a method for the solution of problems in elasticity that takes into account the effect of pore pressure and pore pressure gradients.

Cleary (1958b) considered the relation of earth stresses to hydraulic fracturing, using a method somewhat modified from Lubinski's. The theory of elasticity used is somewhat limited as it assumes linearity of the stress-strain relation. The fact that the stress-strain relation for porous materials is nonlinear is well demonstrated in the experiments reported here.

Compressibility

The unit change in volume per unit change in the pressure applied to the boundary is the compressibility. For porous materials, however, several boundaries may be defined - the external boundary, the pore boundaries, or the external and pore boundaries taken together. Several volumes also may be defined - the gross volume, the volume of the grain material, or the pore volume. Several types of compressibility may be defined for porous materials, depending on what volume the pressure is changing. We will distinguish between the pressure acting on the gross external boundary, σ , and the pore pressure, P.

Grain Compressibility

If an isotropic porous material is immersed in a fluid under pressure, the pressure acts on the outer boundary and throughout the connected pore boundaries, so $\Delta\sigma = \Delta P$.

A change in the pressure results in a change in the gross volume of the material. The grain compressibility, β, is the slope of the volume dilatation versus pressure and is defined by the derivative

$$\beta = \left[\frac{\delta e}{\delta \sigma}\right]_{(\sigma - P) = \text{constant}}$$

where the volume dilatation, e, is brought about by equal changes in the external stress, σ , and the pore pressure, P.

Linear strain, ϵ, is equal to one-third the dilatation, e. Thus, what will be called here the linear compressibility is equal to one-third the volume compressibility. Therefore

$$\left[\frac{\delta \epsilon}{\delta \sigma}\right]_{(\sigma - P) = \text{constant}} = \frac{\beta}{3} \qquad (1)$$

Experimental data will be interpreted in terms of the linear compressibility because strains rather than volume changes are measured directly by the strain gages.

The linear grain compressibility defined by equation (1) is independent of the geometry of the porous structure. It depends directly on the material making up the porous structure.

Bulk Compressibility

If in another experiment the specimen to be tested is given a thin, impermeable coating and the fluid pressure applied, again a uniform strain is produced. This time the pressure, σ , is applied to the external surface and excluded from

the internal pore surfaces. The slope of the strain-versus-pressure curve in this case is the bulk compressibility of the material. The bulk compressibility

$$\left[\frac{\delta e}{\delta \sigma}\right]_{P = \text{constant}}$$

can be expressed in terms of the other bulk elastic constants.

$$\left[\frac{\delta e}{\delta \sigma}\right]_{P = \text{constant}} = 3\left[\frac{1-2\mu}{E}\right]$$

according to the connecting equation given by Timoshenko and Goodier (1951, p. 10). E is Young's modulus for the bulk material, and μ is Poisson's ratio for the bulk material. Linear strain is equal to one-third the volume strain; therefore the linear bulk compressibility is

$$\left[\frac{\delta \epsilon}{\delta \sigma}\right]_{P = \text{constant}} = \frac{1-2\mu}{E} \qquad (2)$$

Hooke's Law

Porous materials such as rock and ceramics have often been treated like the more conventional nonporous elastic materials. It is customary to ignore the fact that the normal stresses are forces per unit area that act discontinuously over a plane passed through the material. A fractional area, n, of a plane passed through the material is occupied by voids; hence, the stresses are average forces per unit gross area. However, even for nonporous materials we must deal with average stresses because there are always microscopic stress fluctuations in real elastic materials.

The conventional form of Hooke's law is

$$\epsilon_x = \frac{\sigma'_x}{E} - \frac{\mu}{E}(\sigma'_y + \sigma'_z) \qquad \text{(cyclic)} \qquad (3)$$

The stress, σ', is the force per unit gross area acting on the solid portions of a plane passed through the material and will be called the solid stress. The stress, σ, is the total force per unit gross area acting on a plane passed through the material and will be called the total stress. The relation between these two kinds of stress is illustrated in figure 1 and given by

$$\sigma_x = \sigma'_x + nP \quad \text{(cyclic)} \qquad (4)$$

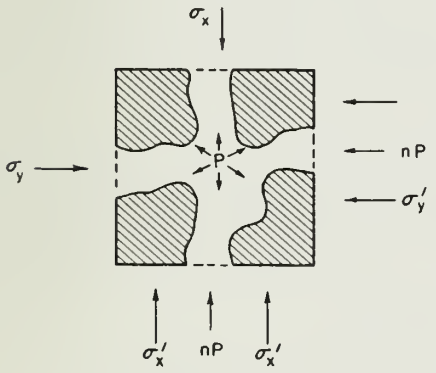

Fig. 1. - Forces acting in two principal directions on an element of porous material.

Equation (3) is a special case of Hooke's Law for porous materials when the pore pressure is zero. However, the presence of fluid pressure in the pores introduces a strain in addition to the strain that is due to the solid stresses, which may be visualized in the following way. The pore pressure, P, while acting on the total

internal boundary of our unit cube in figure 1, is excluded from the solid portions of the external boundary. The effect of such a condition is the same as having the unit cube entirely immersed in a fluid at a pressure, P, and then having a superposed tension normal to the solid portions of the external surfaces of magnitude $-[(1-n)P]$. This equivalence is indicated in figure 2.

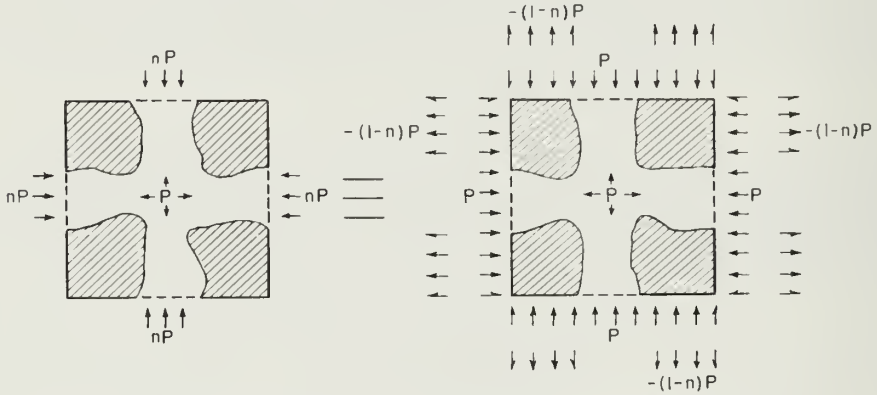

Fig. 2. - Diagram showing equivalence of pore pressure distribution on an element of porous material to the complete immersion of the element, together with a superposed tension on the external solid boundary of intensity:-(1-n)P.

The strain due to complete immersion in a fluid under pressure is the same in all directions and according to (1) is the linear grain compressibility times the change in pressure

$$\left(\frac{\beta}{3}\right) P$$

The strain due to a tension of $-(1-n)P$ on the solid portions of the external boundaries of the unit cube is the linear bulk compressibility, defined by equation (2), times the normal tension at the surface

$$-(1-n)\ \frac{(1-2\mu)}{E}\ P$$

The strain due to the presence of fluid pressure is therefore

$$\left[\frac{\beta}{3} - (1-n)\ \frac{(1-2\mu)}{E}\right] P \qquad (5)$$

The expression for the total strain is then obtained by adding (5) to the right hand term in (3)

$$\epsilon_x = \frac{\sigma'_x}{E} - \frac{\mu}{E}\ (\sigma'_y + \sigma'_z) - \left[(1-n)\ \frac{(1-2\mu)}{E} - \frac{\beta}{3}\right] P \quad \text{(cyclic)} \quad (6)$$

This is a form of Hooke's law for porous materials taking into account the strain due to pore pressure. It was obtained by Lubinski (1954) and is in terms of the solid stress.

A form of Hooke's law for porous materials in terms of the total stress will be obtained from (6) by substituting for the solid stresses, σ'_x, σ'_y, and σ'_z,

their expressions in terms of the total stresses and pore pressure (4). It then becomes

$$\epsilon_x = \frac{\sigma x}{E} - \frac{\mu}{E}(\sigma_y + \sigma_z) - \left[\frac{1-2\mu}{E} - \frac{\beta}{3}\right] P \quad \text{(cyclic)} \qquad (7)$$

Cleary (1958a) noted several advantages in using this form of Hooke's law for porous material. The porosity term does not appear in the expression. The stress is continuous across an impermeable boundary to the porous system. No body force due to fluid motion through the porous material exists in terms of the total stress. Consequently, the analogy suggested by Lubinski (1954) between thermal stresses and stresses resulting from pore pressure distribution is more conveniently applied.

The analogy between thermal stresses and stresses due to pore pressure becomes evident by noting that the strain due to pore pressure is uniform in all directions, as is the strain due to temperature changes. The coefficient of P in (7) has a physical significance analogous to the coefficient of thermal expansion. Therefore, it is natural to define the coefficient of P as a single property of the porous material. Thus

$$J = \left[\frac{1-2\mu}{E} - \frac{\beta}{3}\right] \qquad (8)$$

where J is the coefficient of pore pressure expansion. If we apply this definition, (7) becomes

$$\epsilon_x = \frac{\sigma_x}{E} - \frac{\mu}{E}(\sigma_y + \sigma_z) - JP \quad \text{(cyclic)} \qquad (9)$$

For zero porosity, J equals zero and the pore pressure term in (9) vanishes. The total stress becomes identical to the solid stress and (9) becomes Hooke's law for isotropic nonporous materials.

Effective Stress

The effective stress is a component of the total stress that tends to compact a porous structure, change its resistance to shear, and change its elastic properties by altering its microscopic pore structure. The effective stress is extensively used in the field of soil mechanics (Terzaghi and Peck, 1948, p. 52). It is stated in terms of the total stress and the pore pressure

$$\bar{\sigma}_x = \sigma_x - P \quad \text{(cyclic)} \qquad (10)$$

It is useful to separate the effective stress from the hydrostatic component of the total stress because changes in elastic properties as stress condition changes can be attributed to changes in the effective component. The hydrostatic component, numerically equal to the pore pressure, has negligible effect on the pore geometry and elastic properties.

EXPERIMENTAL PROCEDURE

Apparatus

The pressure cell used in the experiments consisted of a thick, steel cylinder with end closures held in the cylinder by the ram or a large hydraulic press.

The core was cemented to the lower closure of the cylinder and a floating piston was mounted on the upper end of the core (fig. 3). Figure 4, an exploded view of the apparatus, shows the steel cushion plate, 1, that distributes the load from the ram of a hydraulic press to 2, a large brass plunger. A short piston, 3, separates the axial and radial fluid pressures. The test cylinder, 4, shows connections, 5 and 6, through which the axial and radial fluid pressures were controlled and measured. The core, 7, is mounted on the bottom closure, 8, of the cylinder together with the tubing connected to the closure and communicating with the pores of the specimen.

Figure 5 shows the apparatus assembled in the hydraulic press. Tubing connections from top to bottom control the axial stress, the radial stress, and the pore pressure. The wires connecting to the strain-indicating instrument are also visible.

Fig. 4. - Exploded view of apparatus.

Fig. 3. - Core mounted on the lower closure of the test cylinder, with floating piston mounted on upper end.

Strain Measurement

Strains in the rock samples were measured by means of SR-4, A-12-2, bonded wire resistance strain gages. A Baldwin type L portable strain indicator was used to read strain in the gage wire.

SR-4 gages consist of a thin strand of fine cupro-nickel gage wire soldered to larger leads. The gage wire and leads are cemented with nitrocellulose cement to a paper backing. The gage wire normally has a protective coating of red felt lightly cemented over the top, but this felt covering was stripped from the gages for the experiments so that the gage could be smoothly painted over with plastic after it was mounted.

Most SR-4 gages contain a grid of gage wire. At the bends a small fraction of the wire is perpendicular to the gage axis. This introduces an error

because the wire senses some of the strain perpendicular to the gage direction. Ordinarily, this error is unimportant and is ignored. For the present experiments, however, this error would be significant and difficult to correct, so the single strand A-12-2 gage was adopted.

Another advantage in using the A-12-2 gage is its relatively long gage length (1 5/8 inches), which permits the measuring of strain over an appreciable portion of the specimen and thus averages out microscopic strain fluctuations.

To determine the effect of pressure on the readings, gages were mounted on high-purity aluminum and copper rods and subjected to hydrostatic pressure up to 8,000 pounds per square inch. Strain was recorded as a function of the pressure.

Had the gages functioned ideally and given the actual strains in the aluminum and copper as a function of pressure, the linear compressibilities of the two metals would have been measured. For copper this is

$$\frac{\delta \epsilon}{\delta \sigma} = 1.68 \times 10^{-8} / \text{ pound per square inch}$$

and for the aluminum

$$\frac{\delta \epsilon}{\delta \sigma} = 3.14 \times 10^{-8} / \text{ pound per square inch}$$

In actual fact the slope of the strain pressure curve indicated by the gage was for the copper

$$\frac{\delta \epsilon}{\delta \sigma} = .72 \times 10^{-8} / \text{ pound per square inch}$$

and for the aluminum

$$\frac{\delta \epsilon}{\delta \sigma} = 2.23 \times 10^{-8} / \text{ pound per square inch}$$

These results were given the following interpretation.

Assume that if the gage were mounted on a completely incompressible sample the gage would indicate a strain, even though no change in length occurred. This indicated strain would be due solely to the action of the fluid pressure on the gage. If, on the other hand, the gage is mounted on a compressible specimen it will indicate the actual strain in the specimen due to the action of the fluid pressure on the specimen plus a superposed apparent strain due to the action of the pressure on the gage. This fictitious strain divided by the pressure it took to produce it we will call the gage pressure coefficient.

Subtracting the measured from the actual compressibility of copper we obtain as the gage coefficient $.96 \times 10^{-8}$ (indicated tensile strain) inches squared

Fig. 5. - Assembled apparatus in hydraulic press.

per pound. For aluminum the experimental value of the coefficient is $.91 \times 10^{-8}$ inches squared per pound. The significance of this correction is discussed later in this report.

The pressure coefficient determined here for the A-12-2 gage is not the same as those reported in the literature for other gages. Apparently the pressure coefficient varies considerably and must be obtained by experiment for the particular gage used.

Accuracy

Relative pressure measurements were made to an accuracy of about ±10 pounds per square inch. The error in the resulting stresses due to error in pressure measurement is about the same. Error in pressure measurement generally amounted to about ±2 percent of the stress and pressure increments measured in the experiments.

The error due to packing friction is about 1 percent of the pressure difference across the packing of the floating piston. The axial stress always was achieved by increasing the pressure from some lower value before taking a reading. As a result, the packing friction would always act in the same direction.

The error in strain measurement varied widely. The strain-indicating instrument could be read to an accuracy of ±1 micro-inch per inch. The gage accuracy as stated by the manufacturer is ±1 percent of the strain measured. This last error is systematic and would not contribute to the scatter of the data points.

The values of the gage pressure coefficients (see above) probably are significant only in the first decimal place, and for convenience the mean experimental value of

$$.935 \times 10^{-8} \text{ inches squared per pound}$$

is rounded to

$$1 \times 10^{-8} \text{ inches squared per pound}$$

This correction for changes in pressure on the gage generally is small compared to the strain measured in the experiment.

The most serious errors originating in the strain gages result from a shift in the gage zero. Zero shift can result from any of the following causes.

Temperature changes may seriously affect the gage zero but were not important in these experiments. The room temperature was fairly constant and the apparatus too massive to allow important temperature changes to take place over the time interval of a single experiment.

Another important source of difficulty is electrical leakage around the gage due to moisture in the system. Fifty million ohms resistance should be maintained between the gage circuit and ground.

Zero shift of the gage also may be caused by creep of the gage wire relative to its bonding material when the wire is under strain.

A shift in the gage zero, probably from this last cause, at times prevented correlation of strains except within a limited range of stress in which the gage was

allowed to become "normalized." An example of this is found in the strain data from the z gage sample 5, table 2. In going from one set of data to the next, the strains did not change systematically with the increased confining stress. After the gage was allowed to relax within a given range of stress, however, the gage would behave reversibly within a limited range of this stress. The trouble could have been avoided entirely by more thorough curing of the plastic cement.

Perry and Lissner (1955) provide a useful source of information on the technique and limitations of resistance wire strain gages.

Samples

Sample 1 was Spar Mountain ("Rosiclare") Sandstone, heavily cemented with calcite and having a porosity of 1 percent.

Sample 2 was Spar Mountain ("Rosiclare") Sandstone, calcite cemented, with 4 percent porosity.

Sample 3 was Spar Mountain ("Rosiclare") Sandstone, calcite cemented, of 7 percent porosity.

The Spar Mountain ("Rosiclare") is Mississippian in age and a part of the Valmeyer Series in Illinois.

Sample 4 was a conglomerate of unknown age consisting of quartz grains 1 to 2 mm in size. The quartz grains have secondary quartz growth such that all the crystal faces are well developed and visible. This rock is extremely competent, almost pure quartz, and had a porosity of 9 percent.

Sample 5 was St. Peter Sandstone, medium-grained, very friable when wet, almost pure quartz, Ordovician in age, and had a porosity of 16 percent.

Sample 6 was Galesville Sandstone, coarse-grained, nearly pure silica, soft enough to crush in the hand when wet, Cambrian in age, and had a porosity of 22 percent.

Sample Preparation

Sandstone specimens with a fair degree of homogeneity were selected from drill cores, and finished to right cylinders 3.45 inches in diameter and 5 inches long.

Two coats of thermosetting plastic were painted on the cores. The first coat was applied as lightly and quickly as possible and then cured. This procedure kept the imbibition of the plastic into the specimen to a minimum. The coatings were from .01 to .02 inch thick.

After the second coat of plastic had been applied and cured, a very light lathe cut was made with a carbide tool to obtain a smooth surface for gage application.

Plastic also was used in applying the gages. One gage was mounted parallel to the axis of the specimen, and another perpendicular to the axis. A one-half inch entry hole at the bottom of the sample was packed with copper wire to prevent possible collapse or spalling of the sandstone.

The mounted cores were subjected to a vacuum and then kerosene was allowed to enter the core under atmospheric pressure. With this fairly incompressible fluid filling the pores, a uniform pore pressure distribution could be attained in a short length of time when pressure was applied to the core.

Figure 3 shows a mounted specimen cemented to the bottom closure of the

Table 1. - Summary of Experiments

Property determined	Boundary conditions					Identities	Specimens tested
	σ_z	σ_r	P	ϵ_z	ϵ_r		
	lbs. per sq. inch			micro-inch per inch			
E (Young's modulus)	Variable	Constant	0	Variable	Variable	$E = \frac{\Delta\sigma_z}{\Delta\epsilon_z}$	1, 3, 4, 5, 6
μ (Poisson's ratio)	Variable	Constant	0	Variable	Variable	$\mu = \frac{\Delta\epsilon_r}{\Delta\epsilon_z}$	1, 3, 4, 5, 6
$\frac{1-2\mu}{E}$ (Linear bulk compressibility)	$\Delta\sigma_z = \Delta\sigma_r = \Delta\sigma$ Variable		0	Variable	Variable	$\frac{1-2\mu}{E} = \frac{\Delta\epsilon}{\Delta\sigma}$	1, 2, 4, 5, 6
$\frac{\beta}{3}$	$\Delta\sigma_z = \Delta\sigma_r = \Delta P = \Delta\sigma$ Variable			Variable	Variable	$\frac{\beta}{3} = \frac{\Delta\epsilon}{\Delta P}$	4, 6
J (Coefficient of pore pressure expansion)	Constant	Constant	Variable	Variable	Variable	$J = \frac{\Delta\epsilon}{\Delta P}$	5, 6
$\left[\frac{JE}{1-2\mu}\right]$	$\Delta\sigma_z = \Delta\sigma_r = \Delta\sigma$ Variable		Variable	Constant	Constant	$\left[\frac{JE}{1-2\mu}\right] = \frac{\Delta\sigma}{\Delta P}$	4, 5, 6
Z	Constant	Variable	Variable	Variable	Constant	$Z = \frac{\Delta\sigma_r}{\Delta P}$	4, 6

test cylinder. A short brass piston is cemented to the top of the core. By controlling the fluid pressure above and below the short piston at the top of the core, the axial and radial stresses in the specimen were controlled.

The strain-measuring gages were cemented to the core. The soldered wire leads were carried out through the base.

EXPERIMENTAL RESULTS

Application of Hooke's Law

It must be emphasized that equation (9), Hooke's law for porous materials derived earlier, is dependent on linearity of the relation between stress and strain.

In the succeeding discussion, equation (9) is used to relate one elastic property to another and to relate elastic properties to experimental conditions and measurements.

Because the experiments show the elastic properties are themselves functions of the condition of stress, the stress-strain relation is clearly not linear. Therefore, some justification of the use of equation (9) is required.

When sufficiently small changes in stress and strain are observed in a porous material the changes will appear to be linear and follow Hooke's law. Therefore, it is legitimate to apply (9) within a limited range of stress condition. We will therefore assume a set of elastic properties applies to each limited range of stress condition.

To describe the stress condition completely it is necessary to specify the three principal stresses (σ_x, σ_y, and σ_z) and the pore pressure (P). But, as was pointed out on page 9, it is the effective components of these stresses defined by equation (10) that can influence the elastic properties of the porous material.

It would be extremely complicated to express the elastic properties in terms of the effective stresses ($\bar{\sigma}_x$, $\bar{\sigma}_y$, and $\bar{\sigma}_z$) taken in detail. Therefore, it is convenient to assume that the elastic properties can be specified in terms of the mean effective stress given by

$$\bar{\sigma} = \left[\frac{\bar{\sigma}_x + \bar{\sigma}_y + \bar{\sigma}_z}{3}\right] \tag{11}$$

Applying equation (10), together with the experimental condition that $\sigma_x = \sigma_y = \sigma_r$, equation (11) becomes

$$\bar{\sigma} = \left[\frac{\sigma_z + 2\,\sigma_r}{3}\right] - P \tag{12}$$

The experimentally determined elastic properties are subsequently measured and plotted as a function of the mean effective stress, $\bar{\sigma}$, defined by equation (12). To assume that the influences of the three principal effective stresses on the elastic properties can be combined in this manner is a convenient simplification not theoretically justified. The main justification of this assumption is the regularity with which the experimental values of the elastic properties can be plotted against the function, $\bar{\sigma}$.

Table 1 summarizes the experiments performed and the increment ratios defining the properties measured.

Young's Modulus

Table 2 contains the data for the experimental determination of Poisson's ratio, μ, and Young's modulus, E.

In this experiment the pressure of the fluid in the annulus of the apparatus was held constant while the pressure above the floating piston at the top of the specimen was varied. The horizontal stress, σ_r, in the specimen was equal to the annular pressure. The axial stress was obtained from the relation

$$\sigma_z = \frac{p_1 a_1 - p_2(a_1 - a_2)}{a_2}$$

where σ_z is the axial stress, p_1 is the pressure of the fluid above the floating piston, p_2 is the pressure in the annulus, a_1 is the cross section of the cylinder and a_2 is the cross section of the specimen.

The values of σ_r and σ_z were set at initial magnitudes and strain readings taken. σ_z was then changed to a new value holding σ_r constant and new strain readings taken. σ_z was then returned to its former value and strain again measured. If everything worked perfectly and the specimen behaved elastically the final strains measured would be equal to the initial strain readings.

The data in table 2 reveal that the strains do not in general return to their initial values when the specimen is returned to the initial stress condition. These deviations in the strain are of the same order as the expected errors in the experiment so they could not be examined quantitatively, but they reveal that a small amount of inelastic set appears to take place with elastic deformation. Inelastic deformation occurs to a greater extent in the direction of the axial stress.

In several cases in which the inelastic strain was excessive the stress cycle was repeated. Repeating the stress cycle generally resulted in more purely elastic strains.

An example of partly inelastic behavior is shown in the data for sample 5, trial 3, data set 1, in table 2. In trials 1 and 2 the core was loaded so that the axial stress was greater than the radial stress. In trial 3 the axial stress was less than the radial stress.

Under conditions of trials 1 and 2 the core tended to shorten, and the data indicate that the core underwent a small amount of inelastic shortening in adjusting to the stress conditions.

Under the conditions of trial 3 the core tended to lengthen and a noticeable inelastic deformation occurred as the core adjusted itself to the new set of deforming stresses.

Because of this large inelastic strain the stresses were repeated to get a better record of the elastic strain. The core had become somewhat adjusted upon the first application of stress so that the strain resulting from the second application was more elastic.

Trial 3 was performed on the fifth sample, using an entirely different stress combination, to obtain some verification of the hypothesis that mean effective stress alone may be sufficient for describing changes taking place in the elastic properties as the condition of stress changes.

In figure 6 the experimental values of the modulus of elasticity are plotted against mean effective stress for all the samples on which this determination was made. The points plotted for sample 5 are distinguishable according to whether the condition $\sigma_z > \sigma_r$ or $\sigma_z < \sigma_r$ existed during the course of the experiment.

Table 2. - Determination of Young's Modulus, E, and Poisson's Ratio, μ.

Data set	σ_r lbs per sq inch	σ_z lbs per sq inch	ϵ_r micro-inch per inch	ϵ_z micro-inch per inch	ϵ_r micro-inch per inch	ϵ_z micro-inch per inch	$\bar{\sigma}$ lbs per sq inch	E	μ
				SAMPLE 1 - porosity 1 %					
1	500	1460	6175	5981					
	500	2680	6200	5764			1020	5.6×10^6	.116
	500	1460	6175	5980					
2	1200	2000	6072	5899					
	1200	3520	6113	5670			1710	6.7×10^6	.184
	1200	2000	6070	5887					
3	1000	2930	6122	5732					
	1000	5970	6195	5327			2150	7.8×10^6	.188
	1000	2930	6122	5698					
4	2800	3040	5890	5746					
	2800	5770	5958	5432			3340	8.7×10^6	.231
	2800	3040	5882	5742					
5	3000	4850	5908	5541					
	3000	8180	5989	5188			4170	9.6×10^6	.234
	3000	4850	5908	5528					
6	3800	5970	5849	5422					
	3800	8710	5913	5155			4820	10.2×10^6	.232
	3800	5970	5852	5428					
7	5400	5490	5670	5548					
	5400	8540	5742	5225			5940	9.6×10^6	.225
	5400	5490	5670	5539					
8	4800	6770	5757	5377					
	4800	9820	5812	5091			5540	10.7×10^6	.199
	4800	6770	5754	5373					
				SAMPLE 3 - porosity 7 %					
1	500	1465	5785	4784					
	500	2690	5793	4522			1020	4.68×10^6	.031
	500	1465	5785	4784					
2	1200	2000	5589	4735					
	1200	3520	5620	4447			1720	5.48×10^6	.111
	1200	2000	5589	4715					
3	1000	2940	5650	4453					
	1000	6000	5705	3970			2180	6.27×10^6	.113
	1000	2940	5650	4465					
4	2800	3030	5286	4645					
	2800	5780	5358	4192			3330	5.93×10^6	.162
	2800	3030	5280	4668					
5	3000	4850	5300	4373					
	3000	8200	5382	3869			4170	6.65×10^6	.162
	3000	4850	5301	4373					

Table 2. - Continued

Data set	σ_r	σ_z	ϵ_r	ϵ_z	ϵ_r	ϵ_z	$\bar{\sigma}$	E	μ
	lbs per sq inch		micro-inch per inch		micro-inch per inch		lbs per sq inch		
6	3800	5960	5205	4270					
	3800	8710	5262	3882			4970	7.26×10^6	.152
	3800	5960	5202	4265					
7	5400	5470	4980	4434					
	5400	8500	5033	4051			5920	8.18×10^6	.144
	5400	5470	4980	4409					
8	4800	6760	5075	4248					
	4800	9820	5135	3839			5960	7.81×10^6	.137
	4800	6760	5087	4215					
				SAMPLE 4 - porosity 9 % - Trial 1					
1	500	500	1332	1259					
	500	1070	1340	1022			690	2.43×10^6	.025
	500	500	1336	1254					
2	1000	1000	1203	1070					
	1000	1570	1209	911			1190	3.70×10^6	.049
	1000	1000	1200	1060					
3	1500	1500	1118	947					
	1500	1070	1122	803			1566	4.10×10^6	.043
	1500	1500	1114	938					
4	2000	2000	937	932					
	2000	2570	945	808			2190	5.05×10^6	.08
	2000	2000	935	910					
5	2500	2500	878	847					
	2500	3070	889	730			2690	5.38×10^6	.094
	2500	2500	880	826					
6	3000	3000	830	768					
	3000	3570	848	660			3190	5.76×10^6	.076
	3000	3000	840	750					
7	3500	3500	818	690					
	3500	4070	840	598			3690	6.56×10^6	.126
	3500	3500	829	680					
					Trial 2				
1	500	500	857	1800					
	500	1070	860	1594			690	2.83×10^6	.022
	500	500	854	1790					
2	1000	1000	740	1638					
	1000	1570	749	1468			1190	3.52×10^6	.062
	1000	1000	738	1622					
3	2000	2000	588	1415					
	2000	2570	596	1292			2190	4.79×10^6	.063
	2000	2000	589	1407					

Table 2. - Continued

Data set	σ_r	σ_z	ϵ_r	ϵ_z	ϵ_r	ϵ_z	$\bar{\sigma}$	E	μ
	lbs per sq inch		micro-inch per inch		micro-inch per inch		lbs per sq inch		
4	3000	3000	470	1269					
	3000	3570	482	1172			3190	6.07×10^6	.117
	3000	3000	472	1263					
5	3500	3500	420	1209					
	3500	4070	432	1113			3690	6.03×10^6	.116
	3500	3500	422	1206					
6	4000	4000	370	1152					
	4000	4570	380	1076			4190	7.45×10^6	.144
	4000	4000	372	1153					
7	4500	4500	328	1109					
	4500	5070	337	1028			4690	7.00×10^6	.110
	4500	4500	328	1110					
8	6000	6000	179	962					
	6000	6570	189	890			6190	7.86×10^6	.131
	6000	6000	180	963					
			SAMPLE 5 - porosity 16 %						
			Trials 1 and 2, $\sigma_z \geq \sigma_r$						
			Trial 1		Trial 2				
1	1500	1500	1353	1434	1360	935			
	1500	2050	1375	1270	1375	782	1591	3.80×10^6	.131
	1500	1500	1355	1410	1358	915			
2	2000	2000	1240	1362	1245	868			
	2000	2550	1262	1228	1265	738	2091	4.30×10^6	.172
	2000	2000	1241	1355	1242	860			
3	2500	2500	1135	1325	1131	821			
	2500	3050	1154	1200	1150	715	2591	4.84×10^6	.167
	2500	2500	1135	1322	1130	820			
4	3000	3000	1003	1415	1028	785			
	3000	3550	1023	1300	1040	680	3091	5.00×10^6	.141
	3000	3000	1005	1420	1028	782			
5	3500	3500	930	1475	922	770			
	3500	4050	945	1382	941	660	3591	5.30×10^6	.150
	3500	3500	928	1490	927	765			
6	4000	4000	831	1470	833	715			
	4000	4550	844	1375	850	620	4091	5.80×10^6	.160
	4000	4000	830	1470	833	716			
7	4500	4500			747	684			
	4500	5050			765	580	4591	5.35×10^6	.18
	4500	4500			746	683			
8	5000	5000			652	640			
	5000	5550			664	544	5091	5.74×10^6	.13
	5000	5000			651	640			

Table 2. - Continued

Data set	σ_r	σ_z	ϵ_r	ϵ_z	ϵ_r	ϵ_z	$\bar{\sigma}$	E	μ
	lbs per sq inch		micro-inch per inch		micro-inch per inch		lbs per sq inch		
9	5500	5500			566	597			
	5500	6050			585	500	5591	5.56×10^6	.197
	5500	5500			565	601			
10	500	500	1640	1440					
	500	1050	1700	1135			591	1.85×10^6	.17
	500	500	1660	1415					
11	1000	1000	1495	1278					
	1000	1550	1520	1060			1091	2.82×10^6	.12
	1000	1000	1498	1230					
					Trial 3, $\sigma_r \geq \sigma_z$				
			ϵ_r	ϵ_r	ϵ_z	ϵ_z			
1	1000	1000	1496	1478	1230	1315			
	1000	450	1440	1432	1570	1572	900	2.18×10^6	.165
	1000	1000	1472	1479	1318	1321			
2	1500	1500	1349		1208				
	1500	950	1312		1379		1419	3.22×10^6	.200
	1500	1500	1343		1209				
3	2000	2000	1218		1116				
	2000	1450	1190		1260		1919	3.82×10^6	.097
	2000	2000	1211		1128				
4	2500	2500	1108		1055				
	2500	1950	1082		1180		2419	4.36×10^6	.203
	2500	2500	1109		1063				
5	3000	3000	1006		997				
	3000	2450	988		1105		2919	5.19×10^6	.151
	3000	3000	1002		1000				
6	3500	3500	908		948				
	3500	2950	890		1050		3419	5.45×10^6	.158
	3500	3500	904		950				
7	4000	4000	810		885				
	4000	3450	790		989		3919	5.45×10^6	.188
	4000	4000	808		890				
					SAMPLE 6 - porosity 22 %				
			ϵ_r	ϵ_z	ϵ_r	ϵ_z			
1	500	550	1764	1770					
	500	1470	1807	297			670	1.87×10^6	.102
	500	550	1749	1812					
2	1000	1410	1580	1355					
	1000	2950	1648	886			1390	3.16×10^6	.146
	1000	1410	1575	1390					
3	2000	2810	1295	1050					
	2000	4360	1344	611			2530	3.62×10^6	.119
	2000	2810	1292	1025					

Table 2. - Continued

Data set	σ_r lbs per sq inch	σ_z lbs per sq inch	ϵ_r micro-inch per inch	ϵ_z micro-inch per inch	ϵ_r micro-inch per inch	ϵ_z micro-inch per inch	$\bar{\sigma}$ lbs per sq inch	E	μ
4	3900	4100	760	900					
	3900	5640	799	517			4220	4.18×10^6	.106
	3900	4100	760	871					
5	4500	5560	640	580					
	4500	7100	688	171			5110	3.93×10^6	.133
	4500	5560	632	545					
6	5000	5490	510	600					
	5000	7030	545	238			5420	4.28×10^6	.107
	5000	5490	503	595					
7	5500	5740	390	577					
	5500	6970	412	289			5760	4.41×10^6	.093
	5500	5740	382	560					

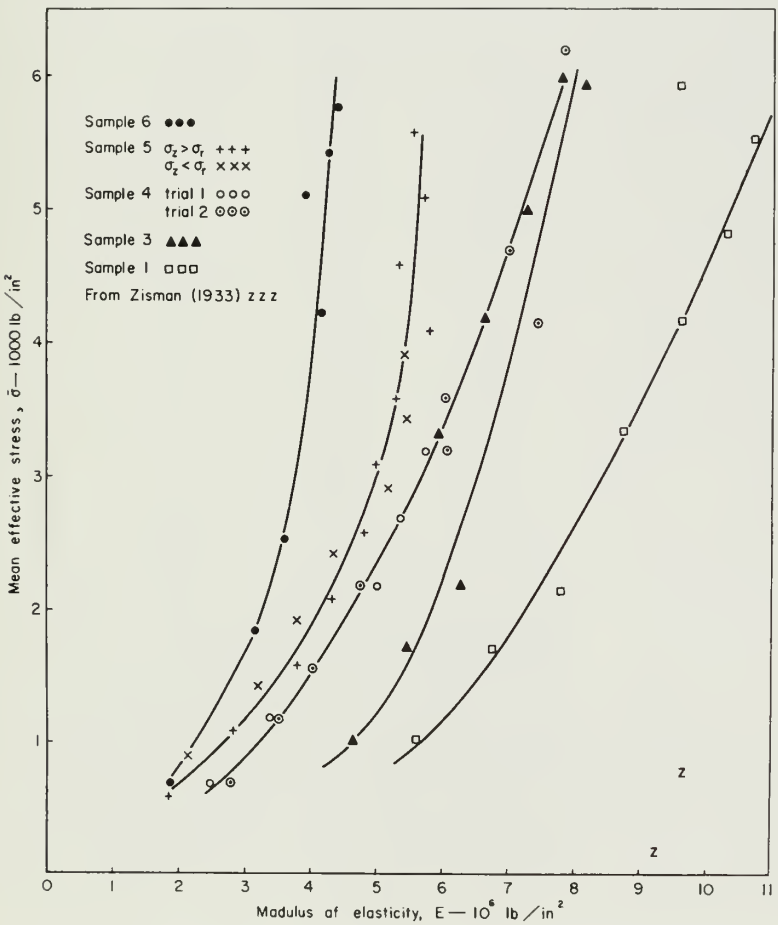

Fig. 6. - Modulus of elasticity as a function of the mean effective stress.

If there is any difference in the traces made by the two sets of points, the difference lies within the scatter of the data. In this case at least, the hypothesis has been verified. Within experimental error it is sufficient to consider changes in elastic properties as a function of the mean effective stress.

The values of Young's modulus plotted in figure 6 correlate fairly well with porosity in spite of the fact that the samples vary widely in age and description. Two of the points are from the work of Zisman (1933a). Zisman's data were obtained by testing at atmospheric conditions a dense quartzitic sandstone.

Poisson's Ratio

Poisson's ratio is the ratio of the radial strain over the axial strain, $\frac{\Delta \epsilon_r}{\Delta \epsilon_z}$, resulting from a change in the axial stress, $\Delta \sigma_z$.

In figure 7 the experimental determinations of Poisson's ratio are plotted.

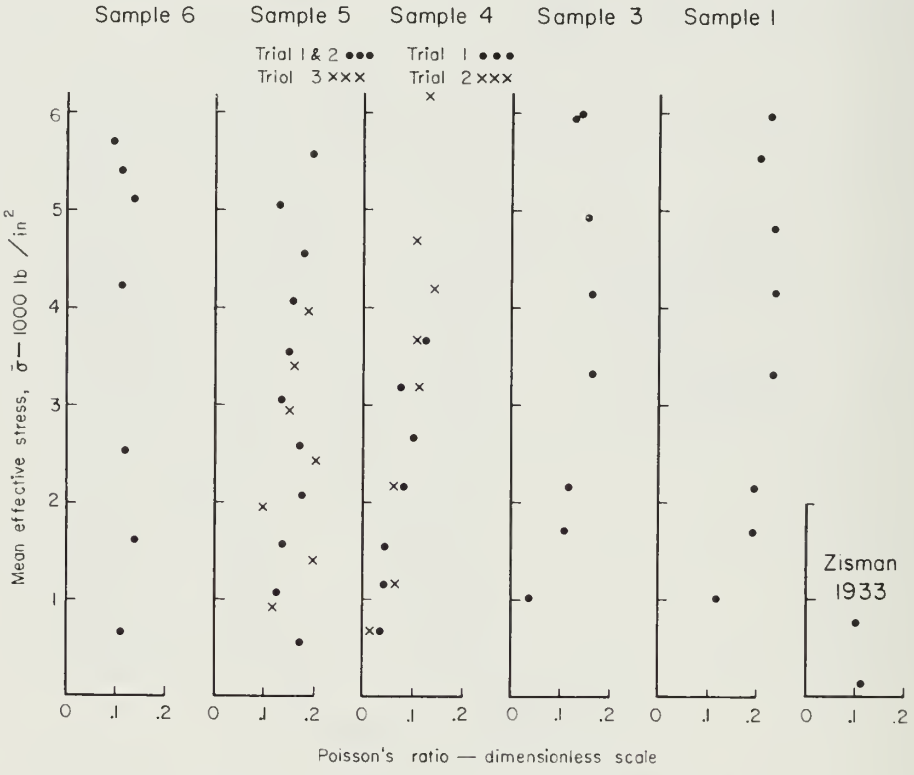

Fig. 7. - Poisson's ratio plotted as a function of mean effective stress.

Data points are widely scattered because the increments of measured horizontal strain are not large compared with the deviations in radial strain caused by inadequate control of the radial stress. An error of 10 pounds per square inch would introduce a radial strain error of about 3 micro-inches per inch, and the strain indicator could be read only within ±1 micro-inch per inch at best. Therefore, the measured horizontal strain increment of about 10 micro-inches per inch was not large compared to the probable errors. The value of Poisson's ratio does not appear

Table 3. - Experimental Values of Poisson's Ratio, μ

Sample	Mean value for $\bar{\sigma}$ <2000 lb/in^2	Mean value for $\bar{\sigma}$ >2000 lb/in^2	Mean of all experimental values
1	.15	.218	.185
3	.071	.145	.108
4	.045	.109	.077
5	.147	.168	.157
6	.124	.112	.118

to change a great deal from one specimen to the next nor does it vary a great deal with the condition of stress in a single specimen.

There is evidently a relation between Poisson's ratio and the mean effective stress. Table 3 shows the mean values obtained when the mean effective stress was less than two thousand pounds per square inch and the mean values under stress conditions greater than two thousand pounds per square inch. With one exception the mean values are greater for conditions of greater mean effective stress.

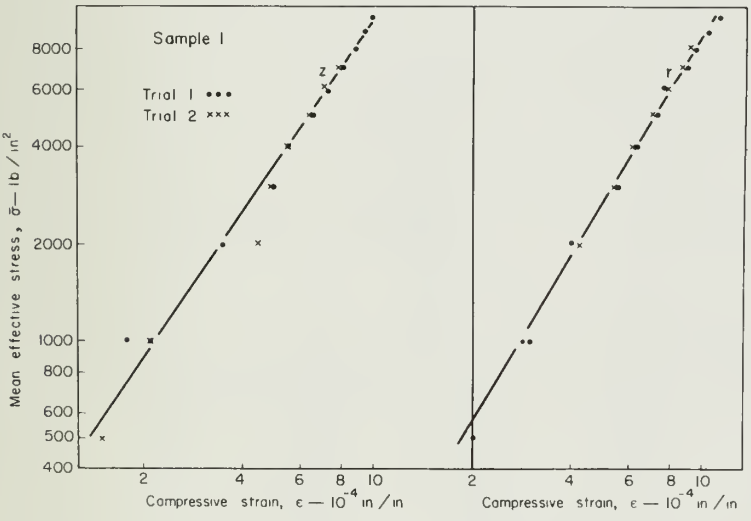

Fig. 8. - Compressive strain is plotted against the mean effective stress in figures 8 to 12. The data in table 3 show tensile strain as positive. The plotted strain readings have been converted so that compressive strain is positive and stress-versus-strain plots as a straight line on logarithmic paper. This was done by subtracting all the strain readings of a single trial from a constant greater than the largest reading. The constant was obtained by trial and error. In figure 8 strain versus mean effective stress is measured by the r and z gages on sample 1.

Obvious correlation between the value of Poisson's ratio and the porosity does not appear.

Linear Bulk Compressibility

Strains due to changes in the external stress, σ, measured while the pore pressure, P, is held equal to zero, are recorded in table 4.

The strain gages are exposed to a change in fluid pressure from one reading to the next, making it necessary to apply the gage pressure coefficient. As explained earlier in this report, the influence of fluid pressure on the gage produced an indicated strain in addition to the actual strain in the specimen.

Table 4. - Determination of Bulk Linear Compressibility, $\frac{1-2\mu}{E}$

SAMPLE 1 - porosity 1%

Trial 1			Trial 2		
$\bar{\sigma}$	ϵ_r	ϵ_z	$\bar{\sigma}$	ϵ_r	ϵ_z
lbs per sq inch	micro-inch per inch	micro-inch per inch	lbs per sq inch	micro-inch per inch	micro-inch per inch
1000	6012	6073	500	6090	6101
2000	5891	5900	2000	5879	5899
4000	5674	5698	4000	5692	5693
6000	5527	5519	6000	5520	5528
8000	5368	5356	8000	5361	5385
10000	5191	5240	7000	5440	5455
9000	5260	5302	5000	5593	5605
7000	5410	5448	3000	5760	5758
5000	5570	5591	1000	5975	6040
3000	5744	5751			
1000	5980	6028			

SAMPLE 2 - porosity 4%

$\bar{\sigma}$	ϵ_r	ϵ_z
lbs per sq inch	micro-inch per inch	micro-inch per inch
400	2775	10127
1000	2507	9899
2000	2286	9819
3000	2158	9654
4000	2040	9475
5000	1958	9367
6000	1840	9201
7000	1740	9067
8000	1630	8966
9000	1522	8814
8000	1650	8949
7000	1850	9078
6000	1825	9219
5000	1959	9333
4000	2081	9489
2000	2343	9800
400	2606	10385

SAMPLE 4 - porosity 9%

$\bar{\sigma}$	ϵ_r	ϵ_z
lbs per sq inch	micro-inch per inch	micro-inch per inch
500	850	1790
1000	729	1620
2000	568	1391
3000	441	1236
3500	386	1172
4000	331	1112
4500	283	1064
6000	119	902

Table 4. - Continued

SAMPLE 5 - porosity 16%

Trial 1, $\sigma_r = \sigma_z$

$\bar{\sigma}$	ϵ_r
lbs per sq inch	micro-inch per inch
500	1640
1000	1472
1500	1339
2000	1220
2500	1110
3000	974
3500	894
4000	790

Trial 2, $\sigma_r = \sigma_z$

$\bar{\sigma}$	ϵ_r
lbs per sq inch	micro-inch per inch
500	1657
1000	1482
1500	1344
2000	1223
2500	1105
3000	998
3500	889
4000	793
4500	701
5000	601
5500	510

Trial 3, $\sigma_r \leq \sigma_z$

$\bar{\sigma}$	ϵ_r
lbs per sq inch	micro-inch per inch
693	1684
1193	1497
1693	1358
2193	1240
2693	1127
3193	991
3693	908
4193	802

Trial 4, $\sigma_r \leq \sigma_z$

$\bar{\sigma}$	ϵ_r
lbs per sq inch	micro-inch per inch
693	1701
1193	1508
1693	1358
2193	1243
2693	1123
3193	1008
3693	904
4193	808
4693	718
5193	612
5693	528

SAMPLE 6 - porosity 22%

$\bar{\sigma}$	ϵ_r	ϵ_z
lbs per sq inch	micro-inch per inch	micro-inch per inch
500	1685	1794
1000	1502	1589
2000	1205	1312
3000	938	1098
4000	676	895
5000	433	695
6000	189	500
7000	-23	310

For example, if the specimen is subjected to a thousand pounds per square inch increase in external pressure, the indicated compressive strain on the instrument is less than the actual value by one thousand times the gage pressure coefficient or ten microinches per inch.

The strain values in table 4 have been corrected for the changes in pressure on the gages. In figures 8 through 12, the stress-versus-strain is plotted on logarithmic paper from the data in table 4. The data have been adjusted to fit an approximately straight line. The empirical equation of each curve was then obtained by assuming that the relation between stress and strain takes the form

$$\epsilon = K_1 \bar{\sigma}^X + K_2 \qquad (13)$$

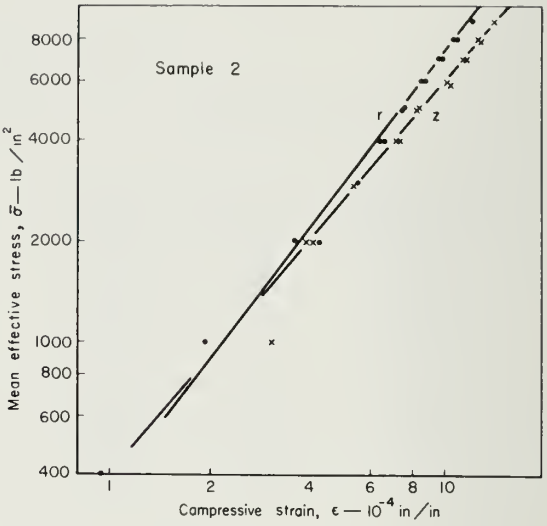

Fig. 9. - Strains measured by z and r gages are plotted versus the mean effective stress for sample 2.

The constant K_2 is a quantity added to each measured value of ϵ to adjust the particular curve to make it plot as a straight line. The application of the first few hundred pounds per square inch of pressure resulted in rather large and unreproducible strains, so strains near zero pressure were not recorded.

The first derivative of the empirical equation (13) gives the bulk linear compressibility as a function of the mean effective stress. Thus

$$\left[\frac{\delta \epsilon}{\delta \sigma}\right]_{P = \text{constant}} = K_1 X \bar{\sigma}^{(X-1)} \qquad (14)$$

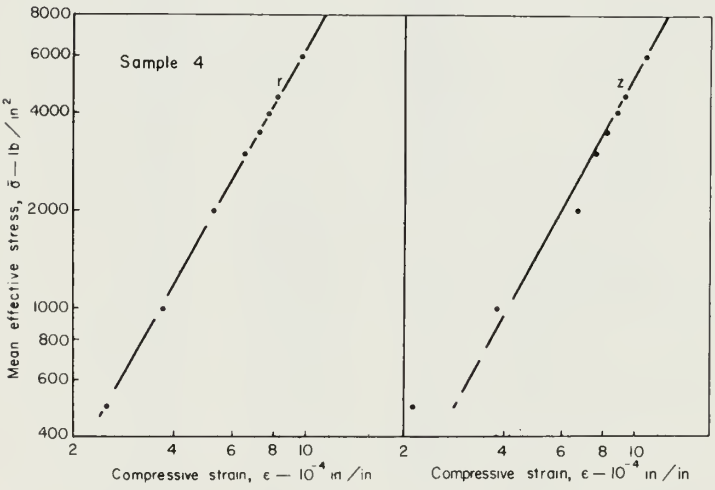

Fig. 10. - Strain measured by z and r gages are plotted versus the mean effective stress for sample 4.

By equation (11) $\delta\bar{\sigma}$ equals $\delta\sigma$ if P is a constant. $\delta\sigma$ has been substituted for $\delta\bar{\sigma}$ on the left side of (14).

The constants K_1 and X for (14) are given in table 5. The empirical equation (14) is plotted in figure 13.

The data of Carpenter and Spencer (1941) also are plotted in figure 13. Carpenter and Spencer measured, while keeping the pore pressure constant, the change in pore volume as a function of the external stress. It was

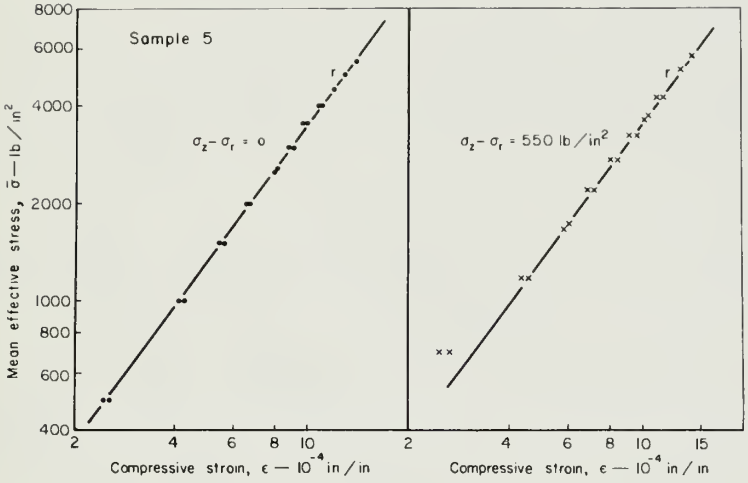

Fig. 11. - Strains measured by the r gage are plotted versus the mean effective stress for sample 5. For the right-hand curve the condition $\sigma_z - \sigma_r = 550$ lb/in^2 is maintained. For the left-hand curve the condition $\sigma_z = \sigma_r$ is maintained. This last condition also obtains for the curves in figures 7 to 10.

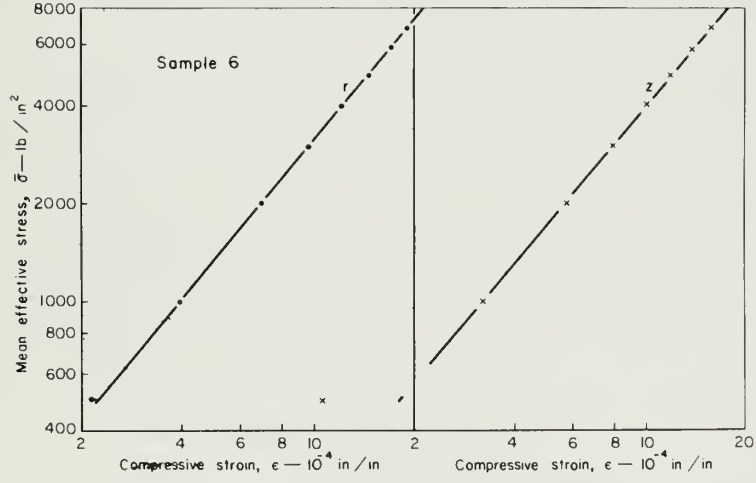

Fig. 12. - Strains measured by z and r gages are plotted versus the mean effective stress for sample 6.

Table 5. - Empirical Constants for Equation (14)

Sample:	1		2		4		5		6	
Gage:	r	z	r	z	r	z	r	z	r	z
$K_1 \times 10^6$	4.86	2.22	1.11	.596	7.70	8.56	2.50		1.42	1.065
X	.585	.664	.763	.852	.558	.555	.740		.814	.826

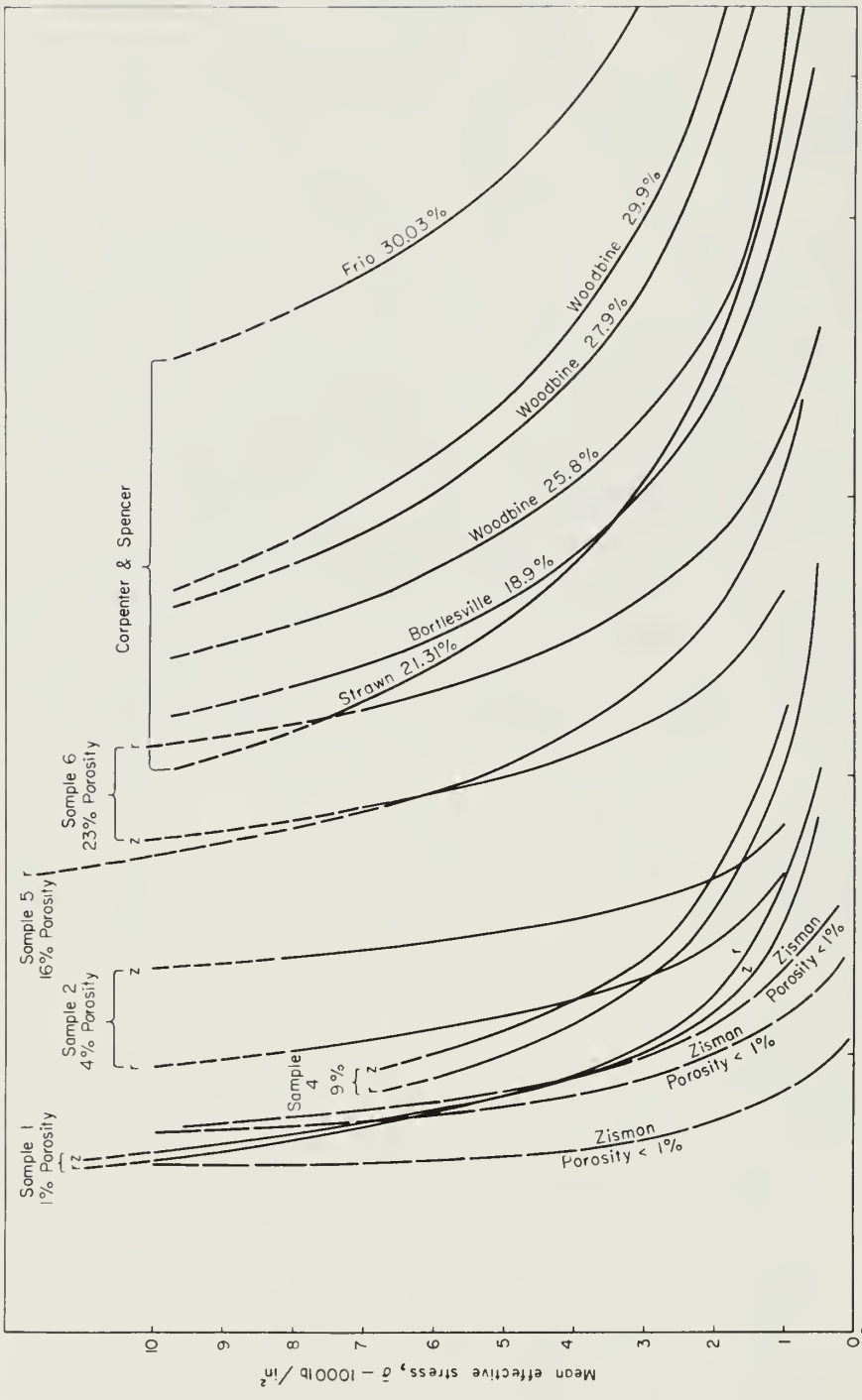

Fig. 13. - The bulk linear compressibility is plotted as a function of the mean effective stress. Curves obtained from the data of Zisman (1933) and Carpenter and Spencer (1941) are included.

therefore necessary to convert their data to the form giving linear bulk compressibility rather than what they called "pore compressibility" as a function of the mean effective stress.

Their data were plotted on logarithmic paper and an empirical equation was obtained in a manner similar to that described above. This empirical equation took the form of (13) and is stated

$$n = K_1 \bar{\sigma}^X + K_2$$

where n is the cumulative change in porosity.
The first derivative gives the rate of change of porosity with mean effective stress

$$\left[\frac{\delta n}{\delta \sigma}\right]_{P = \text{constant}} = K_1 X \bar{\sigma}^{(X-1)} \qquad (15)$$

On the left side $\delta \bar{\sigma}$ has been replaced by $\delta \sigma$. Geertsma (1957) gives the following identity connecting the change in porosity with external stress and the bulk volume dilatation with external stress

$$\left[\frac{\delta e}{\delta \sigma}\right]_{P = \text{constant}} = n\left[\frac{\delta n}{\delta \sigma}\right]_{P = \text{constant}} + \beta \qquad (16)$$

In isotropic materials the linear strains, ϵ, due to a hydrostatic change in stress, are equal to one-third the volume dilatation, e. By dividing the right side of (16) by three and replacing e with ϵ on the left, the relation between the bulk linear compressibility and the "pore compressibility" measured by Carpenter and Spencer is obtained as

$$\left[\frac{\delta \epsilon}{\delta \sigma}\right]_{P = \text{constant}} = \frac{1}{3} n \left[\frac{\delta n}{\delta \sigma}\right]_{P = \text{constant}} + \frac{\beta}{3} \qquad (17)$$

From (15) and (17) the empirical formulae of the bulk linear compressibilities were obtained from Carpenter and Spencer's data. These formulae are plotted in figure 13.

Two correlations are evident in figure 13. The compressibility decreases with decreasing porosity and decreases with mean effective stress.

Carpenter and Spencer's data show this with greater regularity and indicate a higher compressibility for a given porosity than the data presented herein.

Zisman's data for compressibility of a quartzitic sandstone also are plotted in figure 13.

Note that the low porosity specimens seem to approach asymptotically the theoretical compressibility of quartz, which is about 6.2×10^{-8} inches squared per pound.

Another effort was made to confirm the hypothesis that only the mean effective stress need be considered in describing the changes in elastic properties as the condition of stress changes. This time different stress combinations were used. Four trials are given for sample 5 in table 4, in two of which σ_r was held equal to σ_z and the strain was measured as a function of σ. In the other two trials $\sigma_r < \sigma_z$ as the mean stress was varied and the strain measured. Examination of figure 11 will show that the curves for mean effective strain versus stress are about the same for the four trials.

Linear Grain Compressibility

A single quartz crystal, being anisotropic, exhibits two linear compressibilities. The one parallel to the major axis is 4.95×10^{-8}/ pounds per square inch and that perpendicular to the axis is 6.85×10^{-8}/ pounds per square inch.

A nonporous aggregate of randomly oriented quartz grains behaving as a continuous framework (no relative movements at the grain contacts) would exhibit a compressibility equal to the mean compressibility of a single crystal. For quartz this is 6.2×15^{-8}/ pounds per square inch.

Table 6 gives the data obtained for determination of the linear grain compressibilities of two samples. The stress-strain relation is linear. Table 7 summarizes the result.

The fluid pressure to which the gages were exposed changed during the course of this experiment so that it was necessary to apply the gage pressure coefficient correction. The data given in table 6 have been corrected for the pressure on the gage.

The mean values of the compressibilities measured axially and horizontally in the two specimens were a little greater than the theoretical mean value for quartz. The values measured along the axis differed markedly from the values measured with the horizontal gages indicating a nonrandom grain orientation. This is not surprising but it does suggest the use of compressibility measurements as a tool in the determination of the distribution of grain orientation in sandstone.

In trial 1 on sample 4 of the external pressure, σ was held at a value greater than the pore pressure, P. This was also true of the procedure used with sample 6. This procedure should insure a closer fulfillment of the requirement that the porous material behave as a unit without relative movements at grain contacts.

Some difference was noted between the value of the compressibility obtained in trial 1 of sample 4, in which the total stress was greater than the pore pressure, and the value obtained in trial 2, in which the external stress was kept equal to the pore pressure.

Coefficient of Pore Pressure Expansion

The coefficient of the pore pressure term in (9) is defined in terms of the other elastic properties by (8)

$$J = \left[\frac{1 - 2\mu}{E} - \frac{\beta}{3}\right]$$

It follows from (9) that

$$\left[\frac{\delta \epsilon}{\delta P}\right]_{\sigma = \text{ constant}} = -J \qquad (18)$$

The product of J and the change in the pore pressure gives the strain due to changes in the pore pressure, just as the product of the coefficient of thermal expansion and a temperature change gives the strain due to the termperature change. For this reason J was labeled the coefficient of linear pore pressure expansion.

The measurement of J was accomplished by holding the externally applied stresses, σ_z and σ_r, constant and measuring the strains versus pore pressure.

The data for the determination of J are given in table 8. The mean effective stress is calculated from the stress, σ, and the pore pressure, P, for each stress condition.

Table 6. - Determination of Linear Grain Compressibility, β_3

SAMPLE 4 - porosity 9%

Trial 1, $\sigma > P$			Trial 2, $\sigma = P$		Trial 3, $\sigma = P$	
σ	P	ϵ_z	$\sigma = P$	ϵ_z	$\sigma = P$	ϵ_r
lbs per sq inch	lbs per sq inch	micro-inch per inch	lbs per sq inch	micro-inch per inch	lbs per sq inch	micro-inch per inch
1000	500	1272	500	1642	6000	1349
2000	1500	1193	1000	1615	5000	1423
3000	2500	1125	2000	1562	4000	1493
4000	3500	1071	3000	1510	3000	1564
5000	4500	1041	4000	1452	2000	1633
6000	5500	990	5000	1397	1000	1703
5000	4500	1040	6000	1343	1000	1701
4000	3500	1080			2000	1628
3000	2500	1142			3000	1558
2000	1500	1182			4000	1489
1000	500	1237			5000	1419
					6000	1350

SAMPLE 6 - porosity 22%

σ	P	ϵ_r	ϵ_z
lbs per sq inch	lbs per sq inch	micro-inch per inch	micro-inch per inch
500	0	1650	1769
1000	500	1603	1739
2000	1500	1540	1697
3000	2500	1466	1635
4000	3500	1381	1581
5000	4500	1305	1512
6000	5500	1230	1425
7000	6500	1163	1366

Table 7. - Experimental Values of the Linear Grain compressibility, β_3, lb/in^2

	z gage $\sigma > P$	z gage $\sigma = P$	r gage $\sigma = P$
Sample 4	5.3×10^{-8}	5.6×10^{-8}	7.2×10^{-8}
Sample 6		6.1×10^{-8}	7.4×10^{-8}

Table 8. - Determination of the Coefficient of Pore Pressure Expansion, J.

SAMPLE 5 - porosity 16%

σ	P	ϵ_r	ϵ_z	$\bar{\sigma}$
lbs per sq inch	lbs per sq inch	micro-inch per inch	micro-inch per inch	lbs per sq inch
7000	100	315	488	6900
7000	400	348	528	6600
7000	1750	483	632	5250
7000	2950	625	740	4050
7000	3880	740	830	3120
7000	4780	875	946	2220
7000	5500	980	1032	1500
7000	5750	1020	1060	1250
7000	0	310	520	7000

SAMPLE 6 - porosity 22%

Trial 1

σ	P	ϵ_r	ϵ_z	$\bar{\sigma}$
lbs per sq inch	lbs per sq inch	micro-inch per inch	micro-inch per inch	lbs per sq inch
6000	100	270	443	5900
6000	1000	380	531	5000
6000	2000	554	675	4000
6000	3000	720	805	3000
6000	4000	904	955	2000
6000	5000	1102	1149	1000
6000	5500	1223	1295	500

Trial 2

σ	P	ϵ_r	ϵ_z	$\bar{\sigma}$
lbs per sq inch	lbs per sq inch	micro-inch per inch	micro-inch per inch	lbs per sq inch
7000	0	106	410	7000
7000	1200	189	483	5800
7000	2100	325	590	4900
7000	3000	473	708	4000
7000	4000	675	833	3000
7000	5000	822	985	2000
7000	6000	1043	1195	1000
7000	6600	1428	1230	400

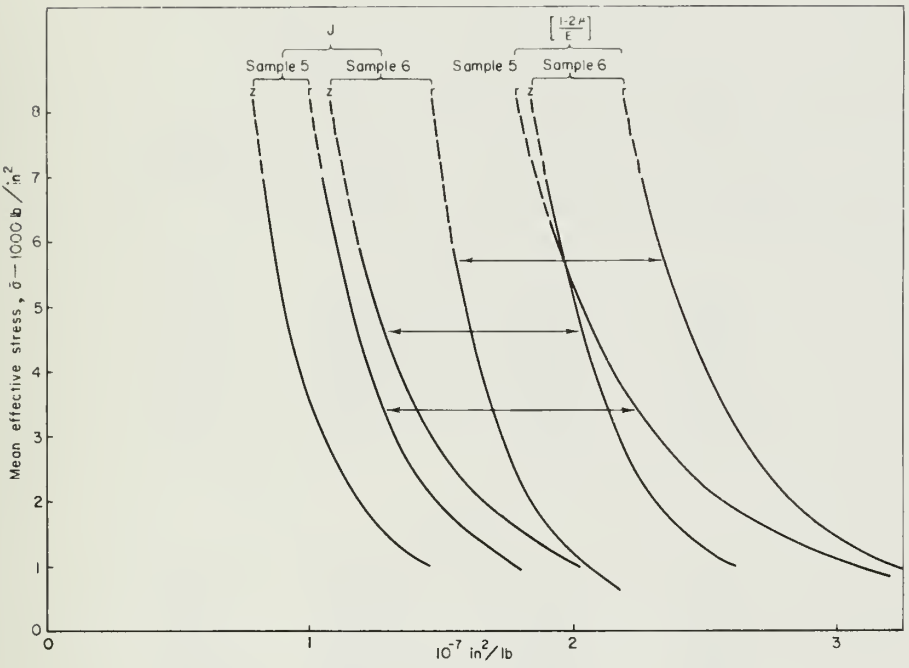

Fig. 14. - The coefficient of pore pressure expansion, J, and the bulk linear compressibilities, $\frac{1-2\mu}{E}$, are plotted against the mean effective stress. Equation (8) predicts that corresponding curves should differ by a constant equal to the grain linear compressibility, $\beta/3$. The figure shows that corresponding curves (indicated by arrows) are spaced horizontally at nearly constant intervals. The intervals are a little greater than the mean linear compressibility of quartz, 6.2×10^8 in^2/lb.

The strains versus the mean effective stress were plotted on logarithmic paper. The strains given in table 8 were subtracted from a larger number selected so that compressive strain would read positive and the points would fall most nearly on a straight line. An empirical equation having the same form as (13) was then obtained from the plotted points. The first derivative of equation (13) is

$$\left[\frac{\delta \epsilon}{\delta \bar{\sigma}}\right]_{\sigma = \text{ constant}} = K_1 X \bar{\sigma}^{(X-1)} \qquad (19)$$

This is about the same method used in handling the data for bulk linear compressibility.

It follows from (11) that if σ is a constant then

$$\delta P = -\delta \bar{\sigma}$$

So, by substituting $-\delta P$ for $\delta \bar{\sigma}$ in the left-hand member of (19), we see that the right-hand member of this equation represents values of J in terms of the mean effective stress.

Table 9. - Determination of $\left[\frac{JE}{1-2\mu}\right]$

SAMPLE 4 - porosity 9%

σ lbs per sq inch	P lbs per sq inch	$\bar{\sigma}$ lbs per sq inch	$\frac{JE}{1-2\mu}$
		Trial 1	
3000	0		
		2570	.45
3700	1550		
		1880	.54
4310	2690		
		1410	.62
4970	3760		
		1070	.77
5860	4920		
		820	.78
6700	6000		
		Trial 2	
4000	0		
		3610	.36
4430	1200		
		2920	.38
4810	2200		
		2300	.40
5210	3210		
		1760	.52
5940	4420		
		1260	.65
6900	5900		
		Trial 3	
1800	0		
		1490	.56
2570	1380		
		1030	.78
3260	2390		
		730	.79
4360	3775		
		460	.84
5670	5340		

$$\left[\frac{\delta\epsilon}{\delta P}\right]_{\sigma = \text{constant}} = -K_1 X \bar{\sigma}^{(X-1)}$$

The empirical equation (19) giving J as a function of the mean effective stress is plotted for each sample in figure 14.

According to (8) the values of J differ from the bulk linear compressibility by a constant, $\beta/3$. To compare theory with experiment, the corresponding experimental curve of the linear bulk compressibility is plotted with J. Note that the differences between the curves are not far from the mean value of the linear grain compressibility of quartz, 6.2×10^{-8}.

Surface Pressure Preventing Expansion Due to Pore Pressure

When an elastic porous material is contained within immovable boundaries, a change in the pore pressure is accompanied by a change in the boundary stress necessary to prevent expansion. By imposing the condition that the three principal

Table 9. - Continued

SAMPLE 5 - porosity 16%

σ lbs per sq inch	P lbs per sq inch	$\bar{\sigma}$ lbs per sq inch	$\frac{JE}{1-2\mu}$
		Trial 1	
2000	175		
		1632	.74
3110	1670		
		1250	.70
3950	2875		
		940	.80
5000	4190		
		740	.79
5530	4860		
		630	.85
6000	5410		
		530	.80
6470	6000		
		Trial 2	
4000	140		
		3660	.52
4750	1285		
		3270	.61
5350	2270		
		3000	.70
5750	2840		
		2750	.59
6200	3610		
		2520	.76
6600	4140		
		Trial 3	
5000	125		
		4660	.64
5730	1275		
		4220	.63
6370	2380		
		3900	.66
6720	2910		

strains are constant, it follows from (9) that

$$\left[\frac{\delta\sigma}{\delta P}\right]_{\epsilon = \text{constant}} = \frac{JE}{1-2\mu}$$

The physical significance of $\frac{JE}{1-2\mu}$ is seen by recalling the analogous thermal stress condition. A change in the temperature of an element confined within immovable boundaries is accompanied by a change in the pressure preventing the expansion of the element. The ratio between the change in the pressure and the change in the temperature is the function $\frac{\alpha E}{1-2\mu}$, where α is the coefficient of thermal expansion.

In order to measure the property $\left[\frac{JE}{1-2\mu}\right]$, the pore pressure, P, and external stress, σ, were varied in such a way that the strain in one gage remained constant. To the extent that the material is anisotropic, a small amount of strain would have occurred in the other gage direction. The theoretical condition of zero strain in all directions was therefore only approximately maintained.

Table 9. - Continued

SAMPLE 6 - porosity 22%

σ lbs per sq inch	P lbs per sq inch	$\bar{\sigma}$ lbs per sq inch	$\frac{JE}{1-2\mu}$
	Trial 1		
2000	175		
		1630	.74
3110	1670		
		1250	.70
3950	2875		
		940	.80
5000	4190		
		740	.79
5530	4860		
		630	.85
6000	5410		
		530	.80
6470	6000		
	Trial 2		
4000	140		
		3660	.52
4750	1285		
		3270	.61
5350	2270		
		3000	.70
5750	2840		
		2750	.59
6200	3610		
		2520	.75
6600	4140		
	Trial 3		
5000	125		
		4660	.64
5730	1275		
		4220	.63
6370	2380		
		3900	.66
6720	2910		

The experimental values of the function $\left[\frac{JE}{1-2\mu}\right]$ are given in table 9. Experimental error resulted in a large scatter in these values.

Fatt (1958b) also evaluated this property indirectly from his compressibility data. His values of $\left[\frac{\delta\sigma}{\delta P}\right]_{\epsilon = \text{constant}}$ are consistent with those given here. However, his measurements are carried all the way to zero stress where the value of $\left[\frac{\delta\sigma}{\delta P}\right]_{\epsilon = \text{constant}}$ approaches one. The measurements in this report were not carried to effective stress much below five hundred psi.

Rate of Change of Horizontal Stress With Pore Pressure in a Porous Sedimentary Bed

If a porous material is restrained from horizontal movement and a constant vertical stress is maintained, the relationship between the pore pressure and the horizontal stress is obtained by imposing these stated conditions on (9). The following relation can then be obtained.

Table 10.- Determination of Z

σ_z lbs per sq inch	σ_r lbs per sq inch	P: lbs per sq inch	$\bar{\sigma}$ lbs per sq inch	Z
		SAMPLE 4 - porosity 9%		
4700	3000	0	3080	.39
4700	3500	1300	2150	.41
4700	4000	2520	1430	.56
4700	4500	3420	960	.71
4700	5000	4130	630	.56
4700	5250	4580		
		SAMPLE 6 - porosity 22%		
		Trial 1		
5700	3500	0	4040	.34
5700	3670	500	3720	.72
5700	4030	1000	3340	.72
5700	4750	2000	2760	.57
5700	5320	3000		
		Trial 2		
6200	3700	100	4100	.52
6200	4220	1100	3500	.68
6200	4900	2100	3050	.71
6200	5400	2800		

$$\left[\frac{\delta\sigma_r}{\delta P}\right]_{\substack{\epsilon_r = \text{constant} \\ \sigma_z = \text{constant}}} = \frac{JE}{1-\mu} = Z \qquad (20)$$

The function $\left[\frac{\delta\sigma_r}{\delta P}\right]_{\substack{\epsilon_r = \text{constant} \\ \sigma_z = \text{constant}}}$ that was expressed in terms of the other elastic properties, $\left[\frac{JE}{1-\mu}\right]$, in Cleary (1958a,b) will here be given the designation, Z, except when necessary to express it in the derivative form. The conditions of horizontal restraint and constant vertical stress are those generally assumed for the petroleum reservoir. Integration of (20) gives the expression for the horizontal stress underground in terms of the pore pressure, P, and the horizontal stress when the pore pressure is zero, σ_{r_o}.

$$\sigma_r = \sigma_{r_o} + ZP \qquad (21)$$

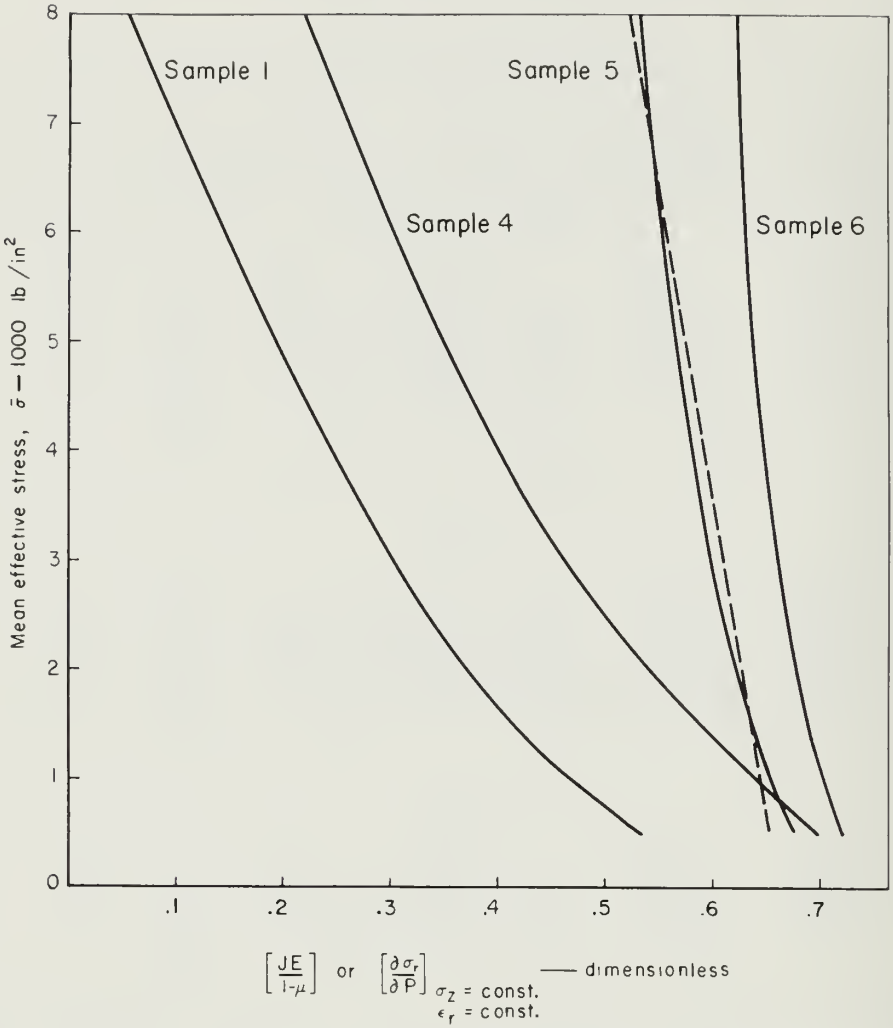

Fig. 15. - The empirical equations for $\frac{\partial \sigma_r}{\partial P}$, where σ_z = constant, ϵ_r = constant, as a function of the mean effective stress are plotted for samples 1, 4, 5, and 6.

The property Z was measured by maintaining constant horizontal strain and axial stress and measuring the horizontal stress as a function of the pore pressure. The data and calculated values of Z are given in table 10.

Unfortunately the errors inherent in the apparatus introduced large errors in this particular experiment. These errors resulted from difficulties in controlling accurately three pressure readings and the reading on the strain indicator at the same time.

One of the principal reasons for performing these experiments was to obtain values of Z. Therefore, empirical equations of this function have been obtained from some of the other experimental data.

Z is expressed in terms of other properties by

$$Z = \left[\frac{1-2\mu}{1-\mu}\right]\left[1 - \frac{\beta/3}{\left[\frac{\delta\epsilon}{\delta\sigma}\right]P = \text{constant}}\right] \tag{22}$$

The bulk linear compressibility, $\left[\frac{\delta\epsilon}{\delta\sigma}\right]P = \text{constant}$, has been expressed in terms of the mean effective stress by (14). The empirical equation (14) together with the mean experimental values of Poisson's ratio and the mean compressibility of quartz can be substituted in (22) to obtain empirical formulae of Z as a function of the mean effective stress for samples 1, 4, 5, and 6. These curves are plotted in figure 15.

The empirical equations obtained for Z take the form

$$Z = \left[\frac{\delta\sigma_r}{\delta P}\right]_{\substack{\epsilon_r = \text{constant} \\ \sigma_z = \text{constant}}} = C_1 + C_2\,\bar{\sigma}^{\,X} \tag{23}$$

In figure 15 it is evident that Z decreases with increasing mean effective stress and that its value decreases with the porosity of the material. The porosities of samples 1, 4, 5, and 6 are respectively 1, 9, 16, and 22 percent.

FRACTURING

The elastic behavior of sedimentary rock is important to the understanding of hydraulic fracture mechanics because the deformation involved in separating the fracture faces during fracture induction is very probably an elastic deformation. In addition, the stresses resisting the propagation of the fracture through the rock are in part the result of elastic behavior. It is this second relationship between the elastic behavior and earth stresses that we concern ourselves with here.

We can with reasonable assurance make the following three statements concerning the extension of hydraulic fractures.

1) The pressure necessary to open and extend a hydraulic fracture approximates the stress in the rock normal to the fracture.

2) Fractures will tend to form in planes normal to the least compressive stress in the rock.

3) The horizontal stress in porous rocks increases with the magnitude of the pore pressure.

Under certain conditions the increase in the horizontal stress as the pore pressure increases is governed by the elastic behavior of the material. The conditions necessary for elastic behavior to obtain are discussed by Cleary (1958a). If the stress condition of the rock does lie within the elastic range, then the change in the horizontal stress with pore pressure is governed by equation (21)

$$\sigma_r = \sigma_{r_o} + ZP$$

This is equation (41) in Cleary (1958a).

It is necessary to assume that Z is a constant in order to apply equation (21). The variation in the value of Z has now been measured as the value of the mean effective stress changes, therefore we will now obtain an equation to replace (21) and take into account the changing value of Z.

Equation (23) is the empirical equation expressing Z as a function of the mean effective stress. We could in principal start with this equation and, by imposing the proper boundary conditions and integrating, obtain the horizontal stress as a function of the pore pressure. The irrational exponent X would make this dif-

ficult in practice, however, so to simplify matters let X equal one and assume a linear relation between Z and the mean effective stress. Such a straight line relation is indicated by the dashed line approximating the experimental values of Z for sample 5 in figure 15. This line will be referred to in a numerical example below.

The derivative form of Z expressed as a linear function of the mean effective stress is

$$\left[\frac{\delta \sigma_r}{\delta P}\right]_{\substack{\sigma_z = \text{constant} \\ \epsilon_r = \text{constant}}} = C_1 + C_2 \bar{\sigma} \tag{24}$$

where C_1 and C_2 are experimentally determined constants.

Substituting the right-hand member of equation (12) we obtain

$$\left[\frac{\delta \sigma_r}{\delta P}\right]_{\substack{\sigma_z = \text{constant} \\ \epsilon_r = \text{constant}}} = C_1 + C_2 \left[\frac{\sigma_z + 2\sigma_r}{3} - P\right] \tag{25}$$

Integration of this equation yields

$$\sigma_r = \frac{3}{2}\left[P - \left(\frac{C_1 + 3/2}{C_2} + \frac{\sigma_z}{3}\right)\right] + C_3 e^{2/3\, C_2 P} \tag{26}$$

This gives us the change in the subsurface horizontal stress as pore pressure changes under the subsurface boundary conditions of constant vertical stress and horizontal strain.

For a specific example assume that a buried porous strata has the elastic properties of sample 5. In figure 15 approximate values of Z for sample 5 are indicated by a dashed line, which is a plot of equation (24). The values of C_1 and C_2 for this particular sample are, respectively, 0.66 and 1.75×10^{-5}.

For example, let σ_z, a constant for all values of P, be equal to 5,000 pounds per square inch. The vertical stress, σ_z, can be computed from the depth of burial of the stratum and the mean density of overlying sediments.

Let the horizontal stress equal 3,000 pounds per square inch when the pore pressure is 2,000 pounds per square inch. It is possible to obtain such information by measuring, respectively, the bottom hole pressure necessary to open a fracture and the bottom hole shut-in pressure.

To obtain the horizontal stress from the fracturing pressure, as just suggested, one assumes that the fracture is vertical. If the fracturing pressure is less than the overburden pressure, as it is in our example, then it may be supposed that the fracture is vertical.

The assumed set of values given in the previous paragraphs have been substituted in (26) to compute the curve (26) plotted in figure 16.

Restrictions on the underground stress conditions due to the negligible tensile strength of large masses of sedimentary rock also are shown in figure 16. They are 45-degree and vertical lines indicating that the horizontal stress, σ_r, can not be less than the pore pressure, P, whereas P can not be greater than the vertical stress, σ_z.

The curvature of line (26) in figure 16 is not great and could have been well approximated by linear relation (21), assuming an average value of Z was selected.

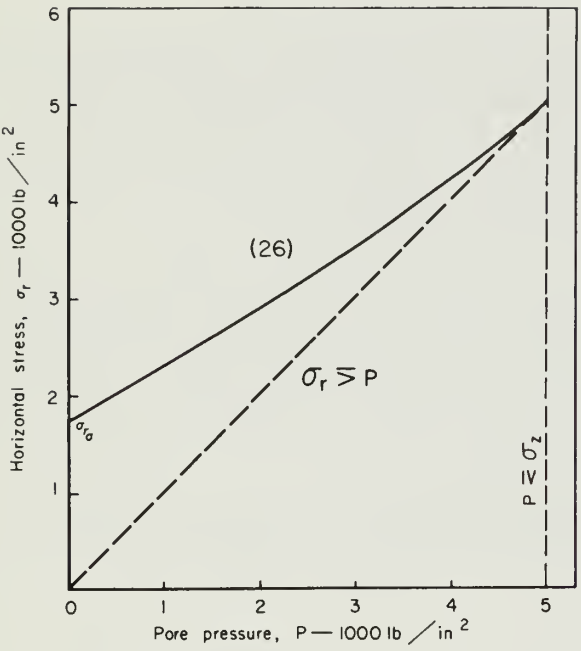

Fig. 16. - The change in horizontal stress with change in pore pressure, calculated for a hypothetical buried porous stratum that has the properties of sample 5.

DISCUSSION AND CONCLUSIONS

The hypothesis which holds that it is sufficient in measuring elastic properties of sandstone to consider the mean effective stress has been tested for validity by plotting the experimentally determined properties against mean effective stress and relating one property to another for a given value of the mean effective stress. Within the limited accuracy of these experiments, it appears that the elastic properties may be treated as functions of the mean effective stress.

As mean effective stress increased, the following regular variation in the elastic properties was observed:

1) The modulus of elasticity increased.
2) The bulk linear compressibility decreased.
3) Poisson's ratio increased, but only slightly.

The rate of change of the horizontal stress in a buried porous stratum as the pore pressure changes has been called Z. Under subsurface conditions, as the pore pressure increases the value of Z increases. Z must always be less than one.

The elastic properties varied from one sample to the next as a moderately regular function of porosity. In general as the porosity decreased

1) the modulus of elasticity increased,
2) the bulk linear compressibility decreased,
3) Poisson's ratio showed no regular variation, and
4) Z approached zero.

If the specimens had been more closely related geologically, a more regular variation in the elastic properties with changes in porosity would have been observed.

Fatt (1958b) has stated that intergranular material such as clay may contribute little or nothing to the elastic structure of the material and yet serve to reduce the porosity. Therefore, the presence of soft intergranular material will fog somewhat the correlation between the elastic properties and porosity.

These experiments have served to show that sandstones have fairly predictable elastic behavior. Further experimental work may make it possible to predict the elastic behavior of buried porous sediments on the basis of lithology, porosity, geologic history, and stress condition.

The increase in the horizontal stress in porous strata as pore pressure increases, predicted in Parts I and II, has been confirmed experimentally.

Hydraulic fracturing pressures generally are less than the computed overburden pressure. It may therefore be supposed that the fractures are vertical. If this is true the fractures are then controlled by the horizontal stress. If the pore pressure is changed within a given zone, the horizontal stress changes and along with it the zone's tendency to fracture. Because the change in the stress may differ from one zone to the next, the vertical extent of the fracture or fractures may be influenced by the pore pressure.

These considerations may be of importance in secondary recovery operations as well as in the stimulation of primary oil production.

REFERENCES

Adams, S. H., and Williamson, E. D., 1923, The compressibility of minerals and rocks at high pressure: Franklin Inst. Jour., v. 195, p. 475-529.

Biot, M. A., 1941, General theory of three dimensional consolidation: Jour. Appl. Physics, v. 12, p. 155-164.

Biot, M. A., 1955, Theory of elasticity and consolidation for a porous anisotropic solid: Jour. Appl. Physics, v. 26, p. 182-185.

Birch, F., 1943, Elasticity of igneous rocks at high temperature and pressure: Geol. Soc. America Bull., v. 54, p. 263-285.

Birch, F., and Bancroft, D., 1938, Effect of pressure on the rigidity of rocks, Parts I, II: Jour. Geology, v. 46, no. 1, p. 59-87, and no. 2, p. 113-141.

Brandt, H., 1955, Study of the speed of sound in porous granular media: Trans. Amer. Soc. Mech. Engrs., v. 22, p. 470-486.

Carpenter, C. B., and Spencer, G. B., 1941, Measurement of the compressibility of consolidated oil bearing sandstones: U. S. Bur. Mines Rept. Inv. 3540.

Cleary, J. M., 1958a, Hydraulic fracture theory, Part I. - Mechanics of materials: Illinois Geol. Survey Circ. 251.

Cleary, J. M., 1958b, Hydraulic fracture theory, Part II. - Fracture orientation and possibility of fracture control: Illinois Geol. Survey Circ. 252.

Dane, E. B., Jr., 1942, Handbook of physical constants: Geol. Soc. America Spec. Paper 36, p. 28.

Fatt, I., 1958a, Pore volume compressibilities of sandstone reservoir rocks: Jour. Petroleum Technology Tech. Note 2004, v. X, no. 3.

Fatt, I., 1958b, Compressibility of sandstones: Am. Assoc. Petroleum Geologists Bull., v. 42, no. 8, p. 1924.

Gassmann, Fritz, 1951, Uber die elastizität poröser Medien: Naturforschenden Gesellshaft Vierteljahrsschrift, Zurich, v. 96, no. 1, p. 1.

Geertsma, J., 1957, Effect of fluid pressure decline on volume changes in porous rocks: Jour. Petroleum Technology, v. IX, no. 12, p. 331.

Hall, H. N., 1953, Compressibility of reservoir rocks: Jour. Petroleum Technology Tech. Note 149, p. 17.

Hubbert, M. K., and Willis, D. G., 1957, Mechanics of hydraulic fracturing: Jour. Petroleum Technology, v. IX, no. 6, p. 153-166.

Ide, J. M., 1936, Elastic properties of rocks, a correlation of theory and experiment: Natl. Acad. Sci.Proc., v. 22, no. 8, p. 482-496.

Lubinski, Arthur, 1954, Theory of elasticity for porous bodies displaying a strong pore structure: Proc. Second U. S. Natl. Cong. Appl. Mech., p. 247.

Perry, C. C., and Lissner, H. R., 1955, The strain gage primer: McGraw-Hill Book Co., New York.

Terzaghi, Karl, and Peck, R. B., 1948, Soil mechanics in engineering practice: Wiley & Sons, New York.

Timoshenko, S., and Goodier, J. M., 1951, Theory of elasticity: McGraw-Hill Book Co., New York.

Zisman, W. A., 1933a, Young's modulus and Poisson's ratio with reference to geophysical applications: Natl. Acad. Sci. Proc., v. 19, no. 7, p. 653-665.

Zisman, W. A., 1933b, Compressibility and anisotropy of rocks at or near the earth's surface: Natl. Acad. Sci. Proc., v. 19, no. 7, p. 680-686.

Illinois State Geological Survey Circular 280
44 p., 16 figs., 10 tables, 1959

CIRCULAR 281

ILLINOIS STATE GEOLOGICAL SURVEY

URBANA